Consideration of Operating Characteristics for Bi-directional LLC Resonant Converter

Sihun Yang*‡, Seiya Abe**, Toshiyuki Zaitsu***, Junichi Yamamoto***,
Masahito Shoyama*, Tamotsu Ninomiya****

*Dep. of Electrical and Electronic Engineering, Faculty of Information Science and Electrical Engineering, Kyushu University

**The International Centre for the Study of East Asian Development

***Texas Instruments Japan Ltd

****Faculty of Engineering, Nagasaki University

yang@ees.kyushu-u.ac.jp, abe@icsead.or.jp, t-zaitsu@ti.com, j_yamamoto@ti.com, shoyama@ees.kyushu-u.ac.jp, ninomiya@nagasaki-u.ac.jp

‡Corresponding Author; Sihun Yang, Dep. Of Electrical and Electronic Engineering, Faculy of Information Science and Electrical Engineering, Kyushu University, Fukuoka, 819-0395, Japan, +81 92 802 3704, yang@ees.kyushu-u.ac.jp

Received: 11.21.2012 Accepted: 03.12.2012

Abstract- In the field of using renewable energy such as the PV system, the batteries are connected to the buses with bi-directional DC-DC converters for ensuring a stable energy supply. Therefore, the bi-directional power conditioners have a key role in renewable power systems. In this paper, bi-directional LLC resonant converter as the power conditioner is proposed. The ac analysis and operating characteristics of bi-directional LLC resonant converter are investigated. Finally, experimental results are shown to confirm the validity of the proposed converter.

Keywords- bi-directional, LLC resonant converter, AC equivalent model, operating characteristics.

1. Introduction

With the depletion of fossil fuel reserves and the increase in pollution, renewable energy systems such as the PV system have been carried out. In these applications, the batteries are connected to the buses with bi-directional DC-DC converters for ensuring a stable energy supply. Therefore, a bi-directional DC-DC converter is one of the most important topics for power electronics [1, 2]. The bi-directional DC-DC converter tends to require high efficiency, low noise and small size etc. The LLC resonant converter is one of the profitable converters to achieve above demands, because of soft-switching operation and simple circuit construction [3-6]. Fig. 1 shows the circuit diagram of bi-directional LLC resonant converter.

In the analysis of the LLC resonant converter, the Fundamental Harmonics Simplification technique (FES) is usually used. So far, the detail analysis of the LLC resonant converter for forward operating mode has been discussed. However, the reverse direction mode of the LLC resonant converter is less well argued so far, and its operating characteristics have not been clarified yet. This paper presents the ac analysis of bi- direction modes by using FES method.

2. Analysis of Resonant Topology

The operating characteristics of resonant network can be evaluated by AC analysis based on the FES method. And it is analyzed by using the f-matrix. The ac equivalent model of the bi-directional LLC resonant converter is shown in Fig. 2 [7].

2.1. AC analysis of Forward Direction Mode

When forward direction mode, the f-matrixes are multiplied from left side of ac equivalent model.

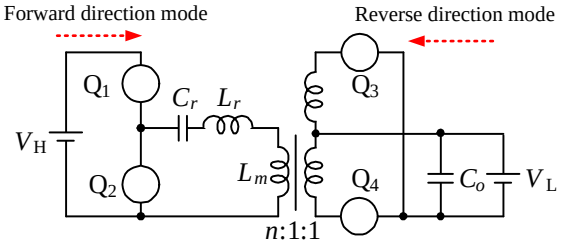

Fig. 1. Bi-directional LLC resonant converter.

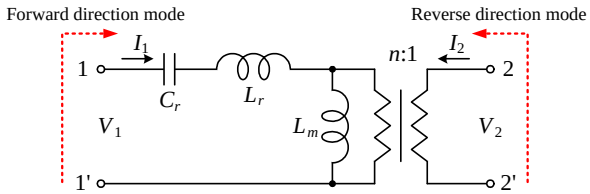

Fig. 2. AC equivalent model of LLC resonant converter.

$$\begin{bmatrix} V_1 \\ I_1 \end{bmatrix} = \begin{bmatrix} 1 & sL_r + \frac{1}{sC_r} \\ 0 & 1 \end{bmatrix} \begin{bmatrix} 1 & 0 \\ \frac{1}{sL_m} & 1 \end{bmatrix} \begin{bmatrix} n & 0 \\ 0 & \frac{1}{n} \end{bmatrix} \begin{bmatrix} V_2 \\ -I_2 \end{bmatrix} \quad (1)$$

The load resistance R_L which connected between port 2-2' of AC equivalent model of the converter is converted AC equivalent resistance as follows ;

$$R_{ac} = \frac{8}{\pi^2} R_L \quad (2)$$

From eq. (1), the operating characteristics of forward direction can be derived as following equations of (3)-(5).

$$Z_{o\_F} = \frac{1}{n^2} \frac{sL_m\left(s^2 L_r C_r + 1\right)}{s^2 (L_m + L_r) C_r + 1} \quad (3)$$

$$Z_{in\_F} = \frac{s^3 L_m L_r C_r + s^2 (L_m + L_r) C_r n^2 R_{ac} + sL_m + n^2 R_{ac}}{s^2 L_m C_r + sn^2 C_r R_{ac}} \quad (4)$$

$$M_F = \frac{s^2 L_m C_r n R_{ac}}{s^3 L_m L_r C_r + s^2 (L_m + L_r) C_r n^2 R_{ac} + sL_m + n^2 R_{ac}} \quad (5)$$

Output impedance: Z_{o_F}, Input impedance: Z_{in_F} and Voltage conversion ratio: M_F

Fig. 3 shows the impedance characteristics and the voltage conversion ratio of forward direction mode using eq. (3)-(5). As shown in Fig. 3 (a), the two resonance peaks of output impedance appear at fsr (series resonant peak) and fpr (parallel resonant peak). On the other hand, only one resonance peak appears between fsr and fpr in the input impedance. One of the advantages of LLC resonant converter is soft switching operation (ZVS turn-on of primary side switches and ZCS turn-off of secondary switches). In order to achieve the soft switching operation, the switching frequency range should be set optimal.

For the ZCS operation of secondary side switches, the range of switching frequency fs is fs<fsr. Moreover, the range of switching frequency fs is fs>fzin (fzin : peak frequency of input impedance) for ZVS operation of primary side switch network. Hence, the range of switching frequency for soft-switching operation (ZVS & ZCS) is fzin<fs<fsr.

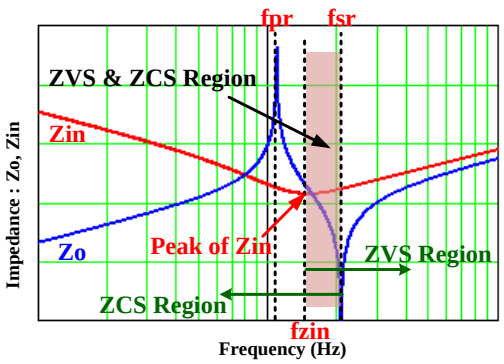

(a) Impedance characteristics

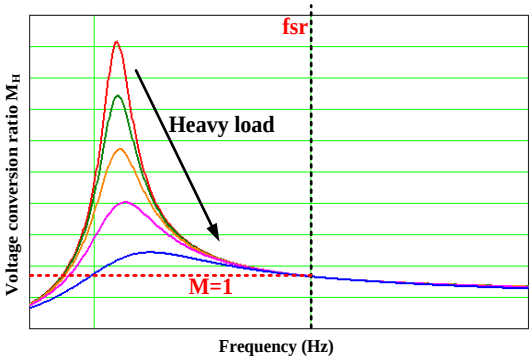

(b) Voltage conversion ratio

Fig. 3. Operating characteristics of the forward direction mode.

As shown in Fig. 3 (b), the peak of conversion ratio of forward direction mode is dumped at heavy load, and the peak frequency is sifted to high frequency side. The movable range of the peak frequency is fpr<fs<fsr. From analysis results, in the forward mode, the operating characteristics depend on load resistance and resonant parameters largely.

2.2. AC Analysis of Reverse Direction Mode

When reverse direction mode, the f-matrixes are multiplied from right side of ac equivalent model.

$$\begin{bmatrix} V_2 \\ I_2 \end{bmatrix} = \begin{bmatrix} \frac{1}{n} & 0 \\ 0 & n \end{bmatrix} \begin{bmatrix} 1 & 0 \\ \frac{1}{sL_m} & 1 \end{bmatrix} \begin{bmatrix} 1 & sL_r + \frac{1}{sC_r} \\ 0 & 1 \end{bmatrix} \begin{bmatrix} V_1 \\ -I_1 \end{bmatrix} \quad (6)$$

In reverse direction mode, the rectifier operation becomes voltage doubler. Therefore, the AC equivalent resistance is derived follows ;

$$R_{ac} = \frac{2}{\pi^2} R_L \tag{7}$$

From eq. (6), the circuit characteristics of reverse direction mode can be derived as following equations of (8)-(10). Output impedance: Zo_R, Input impedance: Zin_R and Voltage conversion ratio: MR

$$Z_{o\_R} = \frac{s^2 L_r C_r + 1}{sC_r} \tag{8}$$

$$Z_{in\_R} = \frac{1}{n^2} \frac{s^3 L_m L_r C_r + s^2 L_m C_r R_{ac} + sL_m}{s^2 (L_m + L_r) C_r + sC_r R_{ac} + 1} \tag{9}$$

$$M_R = \frac{1}{n} \cdot \frac{sC_r R_{ac}}{s^2 L_r C_r + sC_r R_{ac} + 1} \tag{10}$$

Fig. 4 shows the impedance characteristics and voltage conversion ratio of reverse direction mode using eq. (8)-(10). As shown in Fig. 4 (a), only one resonance peaks appears at fpr in the output impedance. On the other hand, there are two resonance peaks appear at fsr (series resonant peak) and fpr (parallel resonant peak) in the input impedance. The frequency of all resonance peaks of both impedance do not depend on load resistance. In reverse direction mode, the frequency range of fs>fsr is good for soft-switching operation (ZVS turn-on of secondary switches). Fig. 4 (b) shows the voltage conversion ratio of reverse direction mode. As shown in Fig. 4 (b), the peak frequency does not change from fsr. Also, the peak voltage conversion ratio does not change, and does not depend on load resistance as well. Furthermore, the voltage conversion ratio does not depend on magnetizing inductance due to eq. (10). Hence, operation near the series resonant frequency fsr is good range for reverse mode.

3. Analysis of Circuit Operation

In this section, the circuit operations of the forward direction mode and the reverse direction mode are investigated in detail, respectively.

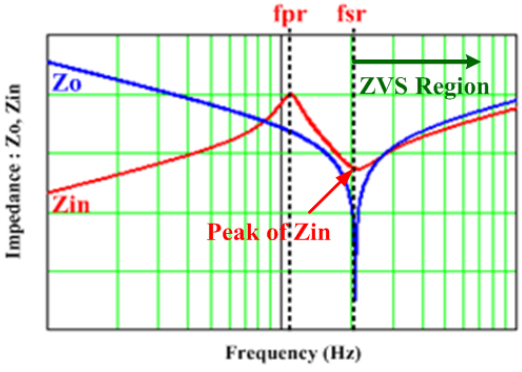

(a) Impedance characteristics

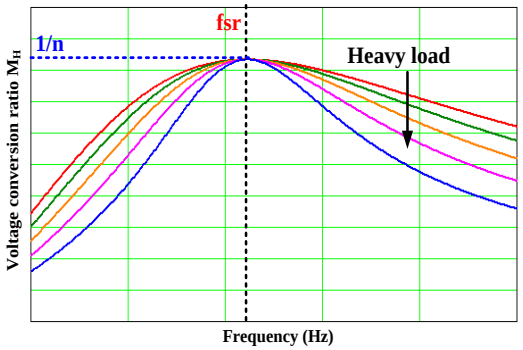

(b) Voltage conversion ratio

Fig. 4. Operating characteristics of reverse direction mode.

3.1. The circuit operation of forward direction mode

The key waveforms and operating states of the forward direction mode are shown in Fig. 5 and 6, respectively. The operating switching frequency is between the series resonant peak fsr and the peak frequency of input impedance fzin in this case. In a half switching cycle, the operation of the LLC resonant converter for forward direction mode can be divided into six states [8-11].

State 1 - This state begins when MOSFET Q_2 turn off. During this period, the current id1 flowing through MOSFET Q_1 is negative, and it discharge Q_1 parasitic capacitor to ensure ZVS operation. This state will be end with the voltage of MOSFET V_{ds1} being zero and the voltage of MOSFET V_{ds2} being the power supply voltage Vin.

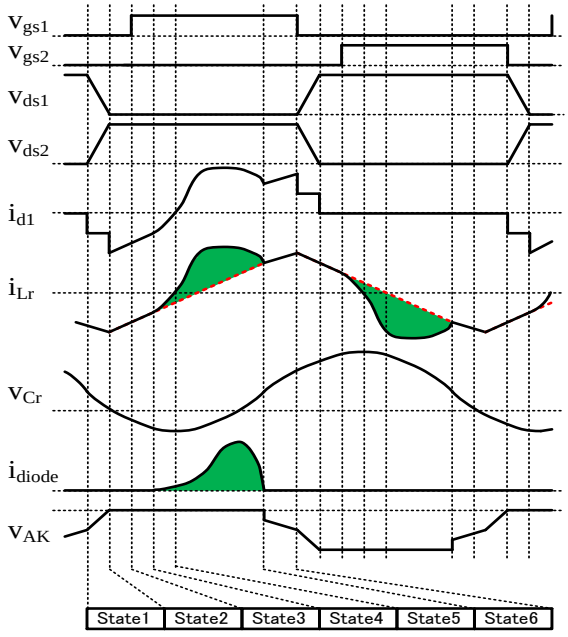

Fig. 5. Operation waveforms of the converter (forward direction mode).

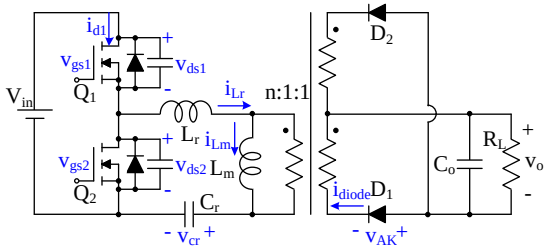

(a) Circuit diagram of the converter

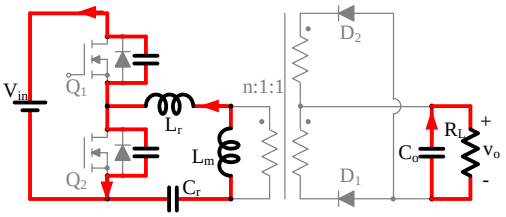

(b) State 1

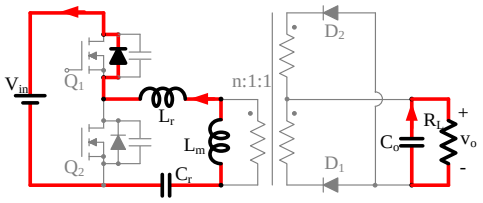

(c) State 2

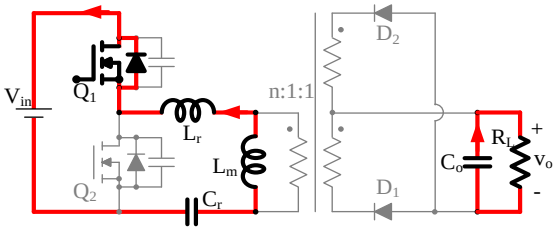

(d) State 3

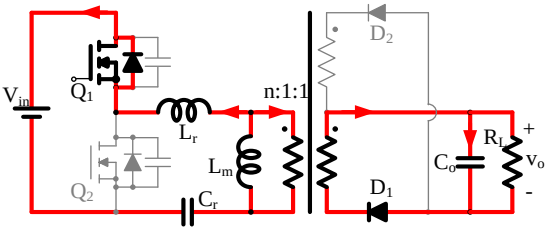

(e) State 4

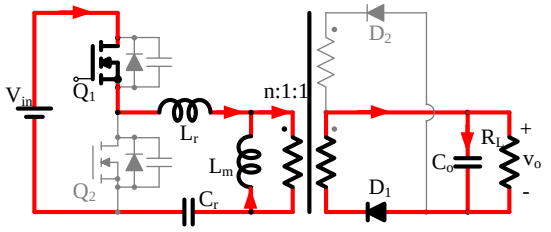

(f) State 5

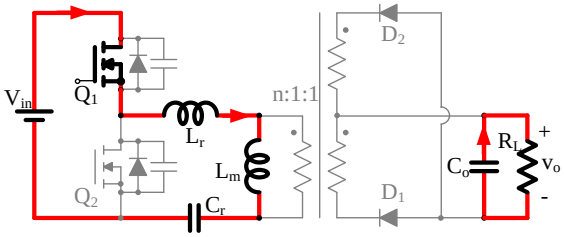

(g) State 6

Fig. 6. Operating mode of LLC resonant converter (forward direction mode).

State 2 - The current id1 flows through the body diode of Q1 in this state. This state will be end when the gate signal of Q1 is inputted.

State 3 - This state starts when Q_1 turns on under the zero voltage. The drain current of Q_1 flows from reverse side because of negative resonant current. The energy stored in the inductance Lr and Lm and the resonant capacitor C_r is fed back to the input terminal, discharging C_r. This state will be end to the resonant current reaches to magnetizing current.

State 4 - When the resonant current reaches to magnetizing current, the diode D1 turns on. In this state, power is fed back to the input side and power is inputted to the output side. This state will be end with the current i_{d1} of Q1 being zero.

State 5 - This state starts when the resonant current i_{Lr} direction is reverse to positive. The current i_{d1} flowing through Q_1 become positive. The energy is supplied from the input terminal, charging C_r.

State 6 - This state starts when the resonant current equal to magnetizing current. The current i_{d1} flowing through D1 become zero. The energy flows from the input terminal, charging C_r and the inductance L_r and L_m.

For the next half switching cycle, the operation is same as analyzed above.

3.2. The Circuit Operation of Reverse Direction Mode

The key waveforms and operating states of the reverse direction mode are shown in Fig. 7 and 8, respectively. The operating switching frequency is higher than the series resonant peak fsr in this case. In a half switching cycle, the operation of the LLC resonant converter for reverse direction mode can be divided into five states.

State 1 - This state begins when MOSFET Q_2 turn off. During this period, the current id1 flowing through MOSFET Q_1 is negative, and it discharge parasitic capacitor of Q_1 to ensure ZVS operation. This state will be end with the voltage of MOSFET V_{ds1} being zero.

State 2 - The current id1 flows through the body diode of Q_1 in this state. The gate signal of Q_1 is inputted to turn on Q_1 under the zero voltage.

State 3 - This state starts when Q_1 turns on under the zero voltage. The drain current of Q_1 flows from reverse side

because of negative resonant current. This state will be end to the resonant current reaches to magnetizing current.

State 4 - When the resonant current reaches to magnetizing current, the diode D_1 turns on. The drain current of Q_1 flows from reverse, continuously. This state will be end to the resonant current reaches to zero.

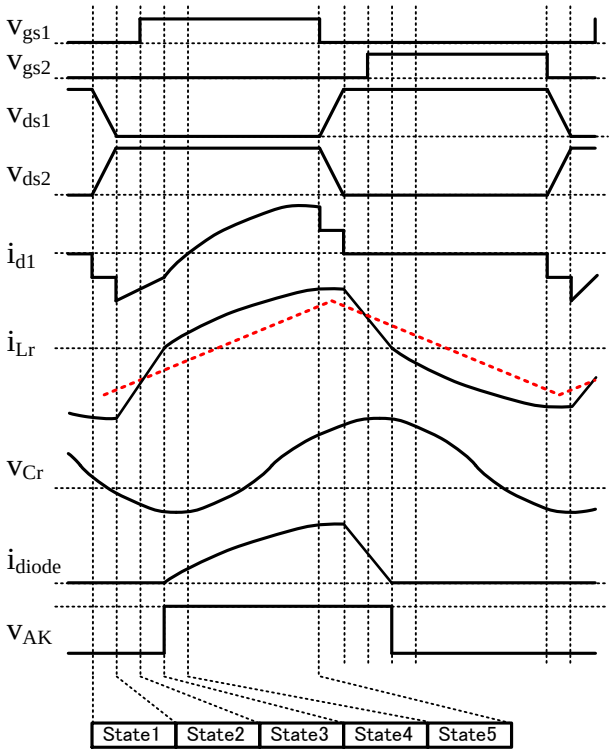

Fig. 7. Operation waveforms of the converter (reverse direction mode).

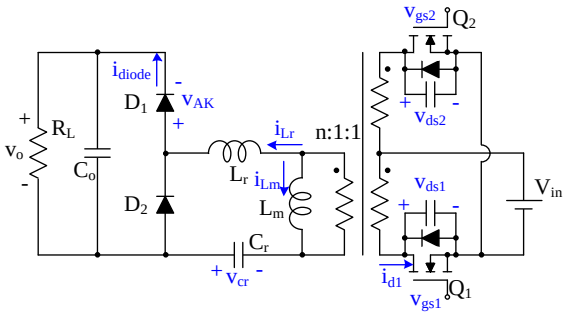

(a) Circuit diagram of the converter

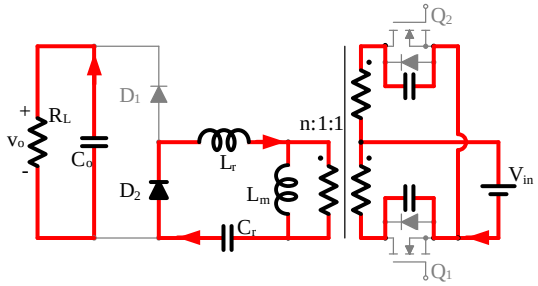

(b) State 1

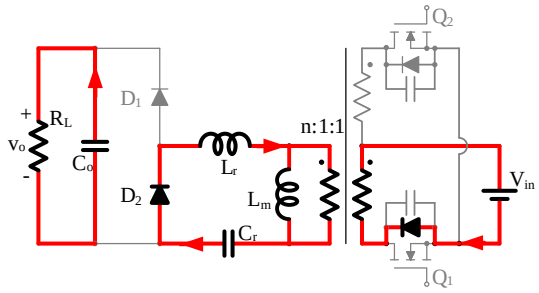

(c) State 2

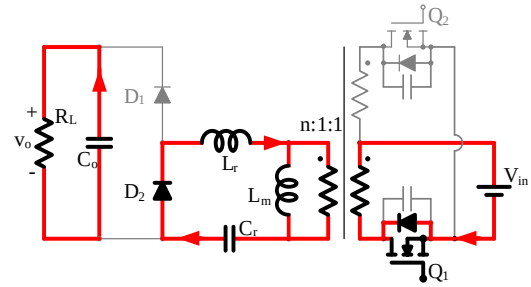

(d) State 3

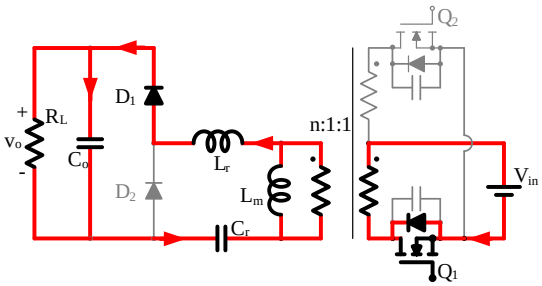

(e) State 4

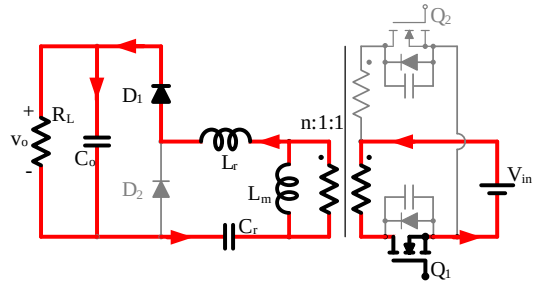

(f) State 5

Fig. 8. Operating mode of LLC resonant converter (reverse direction mode).

State 5 - This state starts when the resonant current i_{Lr} become positive. The current i_{d1} flowing through Q_1 become positive. The energy is supplied from the input terminal, charging the capacitor C_r and is outputted to the output terminal through D_1.

For the next half switching cycle, the operation is same as analyzed above.

4. Experimental Results

In order to clarify validity of operating characteristics of forward and reverse direction modes, the prototype circuit is

implemented. The circuit parameters and specifications are shown in Table 1. In this case, the resonance peak fpr and fsr are around 150kHz and 270kHz, respectively.

4.1. Forward Direction Mode

The output voltage characteristics are measured as shown in Fig. 9. As shown in Fig. 9, the gain peak frequency of voltage characteristics is changed by load resistance.

Table 1. The circuit parameters and specifications.

Signs	Parameters	Value	
		Forward mode	Reverse mode
V_{in}	Input voltage	48V	12V
n	Turns ratio of Transformer	3	
L_m	Magnetizing inductance	37μH	
L_r	Leakage inductance	16μH	
C_r	Resonant capacitance	22nF	

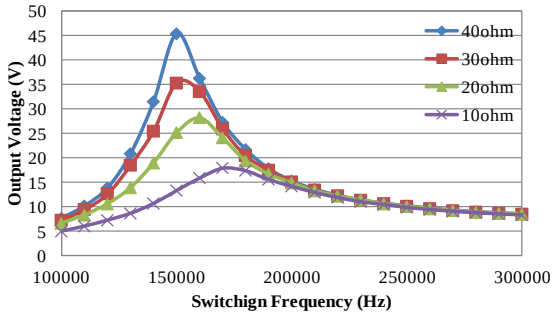

Fig. 9. Voltage gain of forward direction mode.

The peak frequency shifts to high frequency range at heavy load, and the peak value of gain curve decrease at heavy load. These characteristics are the same as analytical characteristics. Figure 10 and 11 show the experimental key waveforms of forward direction mode. The operating condition is 20W load. In this case, the switching frequency is 200 kHz and 300 kHz, respectively. From experimental verifications, the operating frequency range for ZVS operation is fzin<fs<fsr.

4.2. Reverse Direction Mode

The output voltage characteristics are measured as shown in Fig. 12. As shown in Fig. 12, the gain peak frequency of voltage characteristics is not changed by load resistance, and the slop of gain curve is decreased at light load. In this case, the peak frequency is around 270kHz. These characteristics are the same as analytical characteristics. The peak value of voltage gain is slightly changed because the voltage drop is changed by load current.

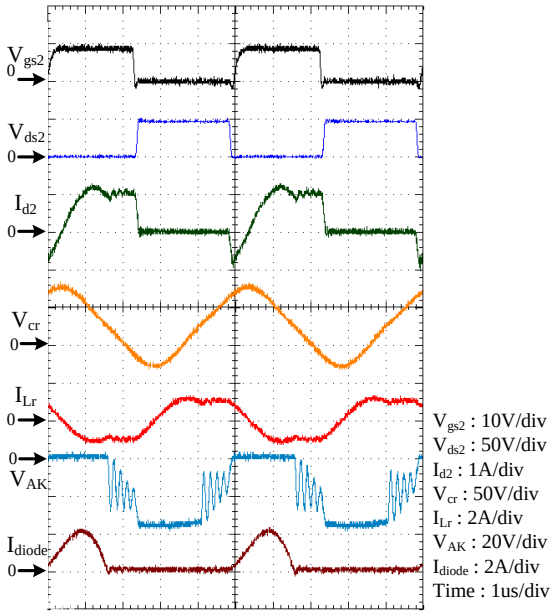

Fig. 10. Experimental waveforms of the converter operating at 200 kHz (fs < fsr)and 20W load for forward direction mode.

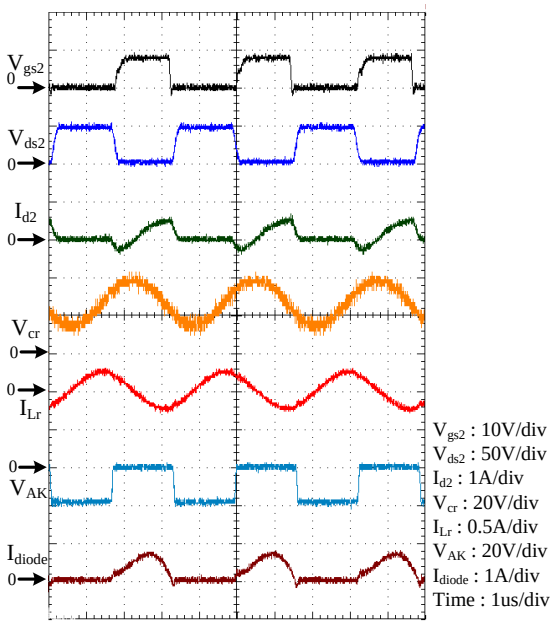

Fig. 11. Experimental waveforms of the converter operating at 300 kHz (fs = fsr)and 20W load for forward direction mode.

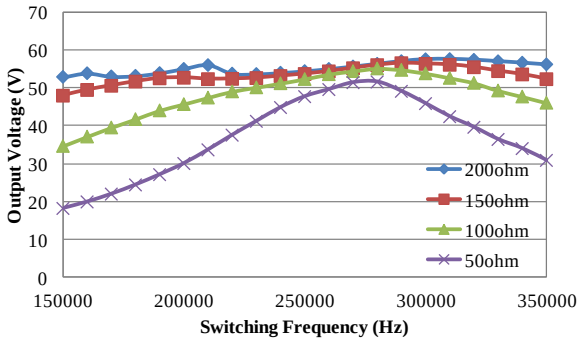

Fig. 12. Voltage gain of reverse direction mode.

Figure 13 and 14 show the experimental waveforms of the converter operating for reverse direction mode. From Fig. 13, the converter operates under ZVS operation when the converter operates at resonant frequency fsr. Also, turn-off surge voltage of switches is close on zero. From Fig. 14, the ZVS operation is confirmed when the converter operates at upper resonant frequency. However, when the converter operates at other frequency except in resonant frequency, turn-off surge voltage of switches is occurred, because the current phase of rectifiers shifts depending on switching frequency.

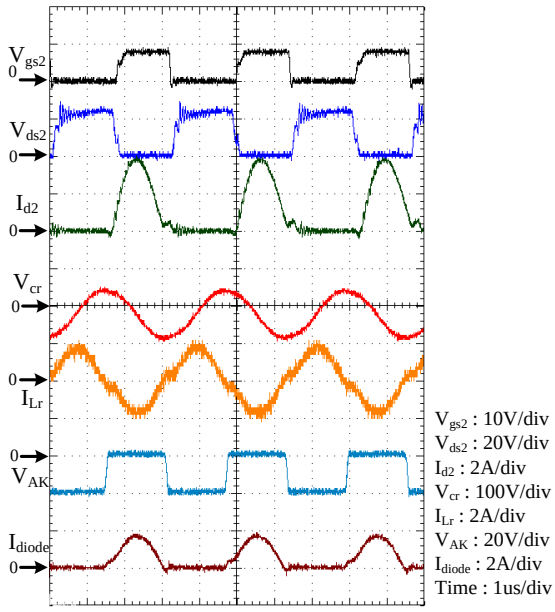

Fig. 13. Experimental waveforms of the converter operating at 300 kHz (fs = fsr)and 100W load for reverse direction mode.

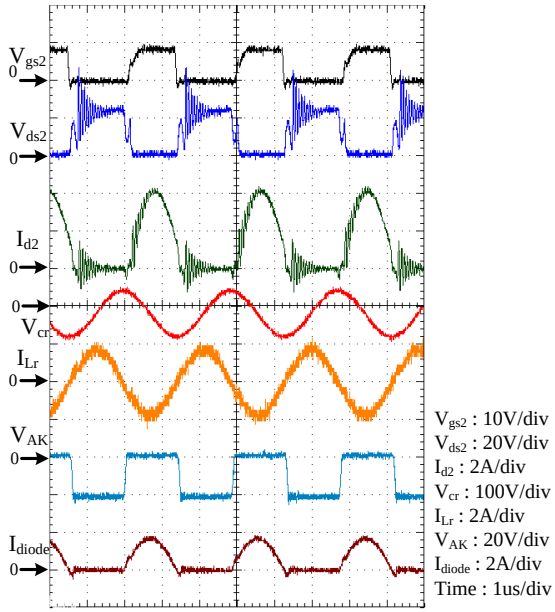

Fig. 14. Experimental waveforms of the converter operating at 350 kHz (fs > fsr)and 100W load for reverse direction mod.

5. Conclusion

In this paper, operating characteristics of bi-directional LLC resonant converter is presented. This paper presents operations and ac analysis of the converter by using FES method. Impedance characteristics and voltage conversion ratio of bi-directional LLC resonant converter is confirmed. Moreover, the circuit operations of bi-direction mode are investigated in detail. From experimental results, it is confirmed that the voltage conversion characteristics are similar to analytical characteristics. From experimental waveforms, the soft-switching operation is confirmed.

References

[1] R. Li, et al, “Analysis and design of improved full-bridge bidirectional DC-DC converter,” IEEE PESC Record, pp. 521-526, June 2004.

[2] S. B. Kjaer, J. K. Pedersen, and F. Blaabjerg, “A review of single-phase grid-connected inverters for photovoltaic modules,” IEEE Trans. Ind. Appl., vol. 41, No. 5, pp. 1292-1306, Sep./Oct. 2005.

[3] M. Jain, M. Daniele, and P. K. Jaine, "A bidirectional DC-DC converter topology for low power application", IEEE Trans. Power electron., vol. 15, no. 4, pp. 595-606, July 2000.

[4] B. Yang, F. C. Lee, A. J. Zhang, G. Huang, “LLC Resonant Converter for front end DC/DC conversion,” in IEEE APEC, pp. 1108-1112, March 2002.

[5] Z. Pavlovic, J. A. Oliver, P. Alou, O. Garcia, J. A. Cobos, "Bidirectional Dual Active Bridge Series Resonant Converter with Pulse Modulation," IEEE APEC, pp. 503-508, February 2012.

[6] J. H. Jung, H. S. Kim, J. H. Kim, M. H. Ryu, J. W. Baek, "High Efficiency Bidirectional LLC Resonant Converter for 380V DC Power Distribution System Using Digital Control Scheme," IEEE APEC, pp. 532-538, February 2012.

[7] S. Abe, T. Zaitsu, J. Yamamoto, T. Ninomiya, “Principle of Overall AC Equivalent Model for Bidirectional Series Resonant DC-DC Converter,” IEEE COMPEL, PS-01-3, June 2012.

[8] K. Morita, “Novel Ultra Low-noise soft-switch-mode Power Supply,” IEEE INTELEC, pp. 115-122, October 1998.

[9] Y. Zhang, D. Xu, K. Mino, K. Sasagawa, “1MHz-1kW LLC Resonant Converter with Integrated Magnetics,” IEEE PESC, pp. 955-961, June 2007.

[10] T. Liu, Z. Zhou, A. Xiong, J. Zeng, J, Ying, "A Novel Precise Design Method for LLC Series Resonant Converter," IEEE INTELEC, pp. 1-6, September 2006.

[11] B. Lu, W. Liu, Y. Liang, F. C. Lee, J. D. van Wyk, "Optimal Design Methodology for LLC Resonant Converter," IEEE APEC, pp. 533-538, March 2006.